

Block Copolymer Nanoparticles Prepared via Polymerization-Induced Self-Assembly Provide Excellent Boundary Lubrication Performance for Next-Generation Ultralow-Viscosity Automotive Engine Oils

Matthew J. Derry,^{*,†} Timothy Smith,[‡] Paul S. O'Hora,[‡] and Steven P. Armes^{*,†}

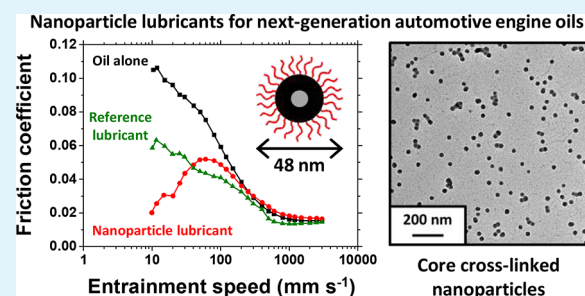
[†]Dainton Building, Department of Chemistry, University of Sheffield, Brook Hill, Sheffield, S3 7HF South Yorkshire, United Kingdom

[‡]Lubrizon Ltd., The Knowle, Nether Lane, Hazelwood, Derbyshire DE56 4AN, United Kingdom

Supporting Information

ABSTRACT: Core cross-linked poly(stearyl methacrylate)–poly(benzyl methacrylate)–poly(ethylene glycol dimethacrylate) [S₃₁–B₂₀₀–E₂₀] triblock copolymer nanoparticles were synthesized directly in an industrial mineral oil via polymerization-induced self-assembly (PISA). Gel permeation chromatography analysis of the S₃₁–B₂₀₀ diblock copolymer precursor chains indicated a well-controlled reversible addition–fragmentation chain transfer dispersion polymerization, while transmission electron microscopy, dynamic light-scattering (DLS), and small-angle X-ray scattering studies indicated the formation of well-defined spheres. Moreover, DLS studies performed in THF, which is a common solvent for the S and B blocks, confirmed successful covalent stabilization because well-defined solvent-swollen spheres were obtained under such conditions. Tribology experiments using a mini-traction machine (MTM) indicated that 0.50% w/w dispersions of S₃₁–B₂₀₀–E₂₀ spheres dramatically reduce the friction coefficient of base oil within the boundary lubrication regime. Given their efficient and straightforward PISA synthesis at high solids, such nanoparticles offer new opportunities for the formulation of next-generation ultralow-viscosity automotive engine oils.

KEYWORDS: block copolymer nanoparticles, polymerization-induced self-assembly, reversible addition-fragmentation chain transfer polymerization, boundary lubrication, tribology



INTRODUCTION

Recently, the automotive industry has seen a concerted drive toward ultralow-viscosity oils because such fluids enable greater fuel economy to be achieved.¹ However, formulating such ultralow-viscosity oils is highly problematic. This is because the addition of oil-soluble polymers, which are normally essential to boost performance and durability, makes it impossible to maintain a sufficiently low overall oil viscosity. In principle, this problem can be addressed by adding polymers in the form of sterically stabilized spherical nanoparticles, which make a negligible contribution to the overall oil viscosity.²

In this context, Liu and co-workers reported that cross-linked acrylic block copolymer nanoparticles can act as boundary lubricants for base oil.³ Lubrication tests performed in a mini-traction machine (MTM) indicated a remarkable reduction in the friction coefficient within the boundary lubrication regime, in which opposing surfaces become sufficiently close to produce frequent metal-on-metal asperity contacts.^{4,5} This typically occurs under high loads and/or when the rate of flow of the lubricating fluid through such

contacts is sufficiently low,³ e.g., for engine start-up at relatively low temperatures. This paradigm-breaking result is potentially highly significant, but unfortunately the synthetic route reported by Liu and co-workers is far from optimal with regard to scale-up.⁶ More specifically, acrylic copolymers are highly susceptible to ester hydrolysis over long time scales within the normal operating temperature of the internal combustion engine (typically 90–120 °C, but up to 250 °C for brief periods under certain conditions).⁷ Moreover, the block copolymer synthesis involved multiple steps and the use of various solvents (toluene, 2-butanone, THF, and pyridine) over the course of a week prior to nanoparticle self-assembly in a Group II base oil at 80 °C for 13 h. Furthermore, the copolymer chains were prepared via atom transfer radical polymerization (ATRP) using a copper catalyst—the deliberate addition of this transition metal is normally considered unacceptable for automotive engine oil applications because its

Received: July 16, 2019

Accepted: August 20, 2019

Published: August 20, 2019

presence is usually taken to be an indication of engine wear.⁸ Any one of these disadvantages is likely to be decisive when assessing the commercial potential of this new approach to boundary lubrication. In combination, there appears to be no realistic prospect of such nanoparticles being utilized on an industrial scale, despite their remarkable performance.

It is well-established that polymerization-induced self-assembly (PISA) enables the efficient synthesis of a wide range of block copolymer nanoparticles directly in many solvents.^{9–12} In particular, PISA formulations have been developed for various non-aqueous media, including alcohols,^{13–21} *n*-alkanes,^{22–29} mineral oil,^{30,31} poly(α -olefins),³⁰ or silicone oils.³² In 2015, we reported that linear block copolymer nanoparticles can be prepared directly in mineral oil using a high-yielding one-pot synthetic route based on methacrylic comonomers, which possess sufficient thermal stability for automotive engine oil applications.³⁰ This protocol involved the initial RAFT solution polymerization of lauryl methacrylate (LMA), followed by the RAFT dispersion polymerization of benzyl methacrylate (BzMA). Well-defined spherical nanoparticles of around 40 nm diameter were obtained at 30% w/w solids within 9 h at 90 °C. More recently, Derry and co-workers found that higher blocking efficiencies and lower dispersities could be achieved using stearyl methacrylate (SMA) instead of LMA.³¹ This latter refinement is used herein to prepare cross-linked sterically stabilized PSMA–PBzMA (herein denoted S–B) nanoparticles in mineral oil (see Scheme 1).

EXPERIMENTAL SECTION

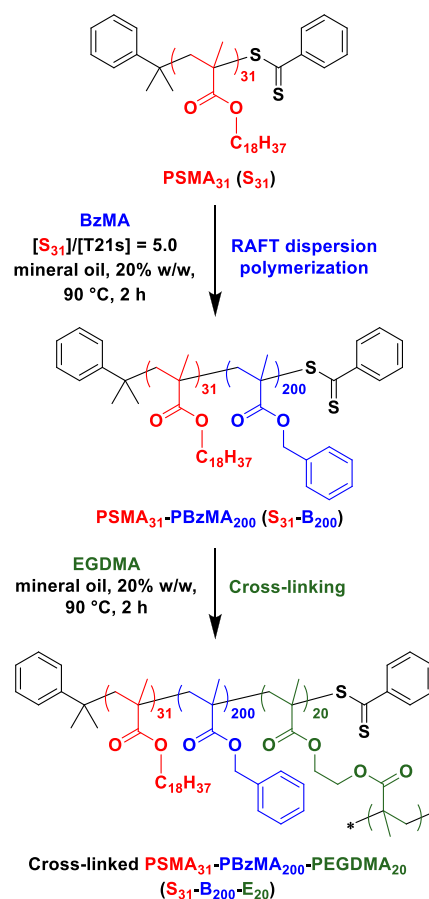
Materials. A 4 cSt American Petroleum Institute (API) Group III mineral oil (2.82% aromatic content) and glyceryl monooleate were kindly provided by The Lubrizol Corporation Ltd. *tert*-Butyl peroxy-2-ethylhexanoate (T21s) initiator was purchased from AkzoNobel (The Netherlands). Cumyl dithiobenzoate (CDB), benzyl methacrylate (BzMA), CDCl₃, and all other reagents were purchased from Sigma-Aldrich (U.K.) and were used as received, unless otherwise noted. Stearyl methacrylate (SMA) was purchased from Santa Cruz Biotechnology (Heidelberg, Germany). THF, *n*-heptane, and toluene were purchased from Fisher Scientific (U.K.). CD₂Cl₂ was purchased from Goss Scientific (U.K.).

Synthesis of Poly(stearyl methacrylate) Macromolecular Chain Transfer Agent (mMacro-CTA) via RAFT Solution Polymerization of Stearyl Methacrylate. The synthesis of the poly(stearyl methacrylate) (S₃₁) macro-CTA has been previously reported by Derry et al.³¹

Synthesis of Poly(stearyl methacrylate)–Poly(benzyl methacrylate)–Poly(ethylene glycol dimethacrylate) Triblock Copolymer Spheres via RAFT Dispersion Polymerization. The synthesis of core cross-linked triblock copolymer spheres via RAFT dispersion polymerization at 20% w/w solids was conducted as follows. Benzyl methacrylate (BzMA; 2.29 g; 13.0 mmol), T21s initiator (2.82 mg; 13.0 μ mol; dissolved at 10.0% v/v in mineral oil), and S₃₁ macro-CTA (0.7 g; 65.0 μ mol; macro-CTA/initiator molar ratio = 5.0; target PBzMA DP = 200) were dissolved in mineral oil (11.96 g). The reaction mixture was sealed in a 50 mL round-bottomed flask and purged with nitrogen gas for 30 min. The deoxygenated solution was then placed in a preheated oil bath at 90 °C and stirred magnetically. After 2 h (BzMA conversion = 98%; M_n = 28.0 kg mol⁻¹, M_w = 34.0 kg mol⁻¹, M_w/M_n = 1.22), ethylene glycol dimethacrylate (EGDMA; 0.245 mL, 1.30 mmol; target PEGDMA DP = 20) and additional mineral oil (1.03 g) were added, and the resulting dispersion was stirred at 90 °C for a further 2 h to afford a 20% w/w dispersion of core cross-linked S₃₁–B₂₀₀–E₂₀ spheres in mineral oil.

¹H NMR Spectroscopy. ¹H NMR spectroscopy studies were conducted as previously reported by Derry et al.³¹

Scheme 1. Synthesis of Poly(stearyl methacrylate)–Poly(benzyl methacrylate)–Poly(ethylene glycol dimethacrylate) (S₃₁–B₂₀₀–E₂₀) Triblock Copolymer Spheres via (i) RAFT Dispersion Polymerization of Benzyl Methacrylate (BzMA) in Mineral Oil at 90 °C Followed by (ii) Core Cross-Linking via Addition of Ethylene Glycol Dimethacrylate (EGDMA)



Gel Permeation Chromatography (GPC). GPC analyses were conducted as previously reported by Derry et al.³³

Dynamic Light-Scattering (DLS). DLS studies were performed at 25 °C using a Zetasizer NanoZS instrument (Malvern Instruments, U.K.) at a fixed scattering angle of 173° as previously described by Derry et al.³¹ Copolymer dispersions were diluted to 0.10% w/w using either *n*-heptane (viscosity at 25 °C = 0.39 mPa·s) or THF (viscosity at 25 °C = 0.46 mPa·s) prior to light-scattering studies.

Transmission Electron Microscopy (TEM). TEM analysis was conducted as previously reported by Derry et al.³¹

Small-Angle X-ray Scattering (SAXS). SAXS analyses were conducted as previously reported by Derry et al.³³ SAXS patterns were recorded over a q range of $0.003 \text{ \AA}^{-1} < q < 0.13 \text{ \AA}^{-1}$ (sample-to-detector distance 5.104 m), where $q = (4\pi \sin \theta)/\lambda$ is the length of the scattering vector and θ is one-half of the scattering angle.

Lubrication Testing. Stribeck curves were obtained using a PCS Instruments mini-traction machine (MTM) consisting of a 19.05 mm diameter steel ball and a 46 mm diameter steel disk. The steel ball and disc are driven independently to create a rolling/sliding contact ratio or slide-to-roll ratio (SRR) of 1:5 (20%) at a constant applied load of 35 N. Tribology measurements were conducted at entrainment speeds ranging from 10 to 3000 mm s⁻¹ using a 4 cSt API Group III mineral base oil in either the presence or absence of 0.5% w/w additives at 100 °C.

Viscosity Measurements. The measurements were performed using an Anton Paar MCR502 rheometer equipped with a Peltier

temperature controller and stainless steel concentric cylinder geometry (28.910 mm cup diameter, 26.656 mm bob diameter, 40.009 mm bob length). The solution viscosity was measured as a function of shear rate at a fixed temperature of either 25 or 100 °C.

RESULTS AND DISCUSSION

RAFT dispersion polymerization in mineral oil at 90 °C was used to prepare core cross-linked poly(stearyl methacrylate)–poly(benzyl methacrylate)–poly(ethylene glycol dimethacrylate) (S_{31} – B_{200} – E_{20}) triblock copolymer spheres, according to Scheme 1. GPC traces recorded for the S_{31} macro-CTA and the corresponding linear S_{31} – B_{200} diblock copolymer precursor are shown in Figure 1. Narrow molecular weight distributions

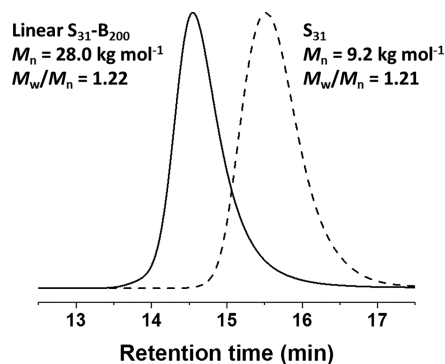


Figure 1. GPC curves [refractive index detector; THF eluent; expressed relative to a series of poly(methyl methacrylate) calibration standards] recorded for the poly(stearyl methacrylate) (S_{31}) macro-CTA synthesized via RAFT solution polymerization in toluene (dashed line) and the linear poly(stearyl methacrylate)–poly(benzyl methacrylate) (S_{31} – B_{200}) diblock copolymer precursor prepared via RAFT dispersion polymerization in mineral oil (solid line).

were obtained in both cases, and a high blocking efficiency (>95%) was achieved for the RAFT dispersion polymerization of benzyl methacrylate in mineral oil at 90 °C. These data indicate excellent RAFT control, as expected for this PISA formulation.³¹

TEM studies of the linear and core cross-linked nanoparticles confirmed a well-defined spherical copolymer morphology in both cases (see Figure 2a and 2b). This technique can only visualize the nanoparticle cores - the poly(stearyl methacrylate) stabilizer chains cannot be detected. DLS was used to examine the particle size distributions of dispersions of the precursor S_{31} – B_{200} spheres and final S_{31} – B_{200} – E_{20} spheres after a 40-fold dilution with *n*-heptane (see Figure 2c). This technique determines the overall hydrodynamic size of the nanoparticles, which includes the steric stabilizer layer. These linear and cross-linked nanoparticles exhibited intensity-average diameters of 42 and 48 nm, respectively. In both cases relatively narrow size distributions were obtained (DLS polydispersity index <0.05). Diluting the core cross-linked S_{31} – B_{200} – E_{20} spheres using THF rather than *n*-heptane prior to DLS studies led to the formation of highly swollen nanogels with an intensity-average diameter of 78 nm. The latter observation confirmed successful core cross-linking using the EGDMA comonomer: if cross-linking had been unsuccessful then nanoparticle dissolution would have occurred to produce molecularly-dissolved copolymer chains because THF is a good solvent for both blocks. TEM analysis of grids prepared using the same dilute nanoparticle dispersion in THF provided further evidence for successful cross-linking

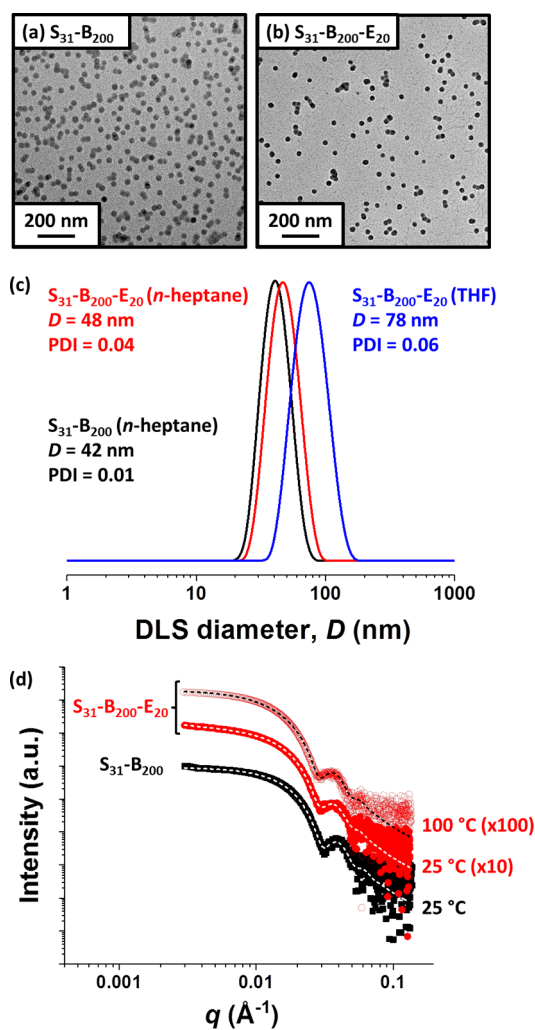


Figure 2. Transmission electron micrographs recorded for (a) linear poly(stearyl methacrylate)–poly(benzyl methacrylate) (S_{31} – B_{200}) spheres and (b) core cross-linked poly(stearyl methacrylate)–poly(benzyl methacrylate)–poly(ethylene glycol dimethacrylate) (S_{31} – B_{200} – E_{20}) spheres. (c) DLS particle size distributions obtained for 0.10% w/w dispersions of linear S_{31} – B_{200} spheres prepared using *n*-heptane as diluent (black data) and core cross-linked S_{31} – B_{200} – E_{20} spheres prepared using either *n*-heptane (red data) or THF (blue data) as diluent. (d) SAXS patterns recorded for 1.0% w/w dispersions of linear S_{31} – B_{200} spheres in mineral oil at 25 °C (black squares) and core cross-linked S_{31} – B_{200} – E_{20} spheres in mineral oil at 25 °C (red circles) and 100 °C (open red circles). Dashed lines represent data fits using an established spherical micelle model.³⁵ For clarity, SAXS patterns are offset by an arbitrary factor, as indicated.

(see Figure S2). Such covalent stabilization is believed to be essential for automotive engine oil applications because it substantially enhances the structural integrity of the nanoparticles under demanding conditions, particularly high temperatures.³ Indeed, it is known that the solvophobic PBzMA block can become sufficiently plasticized on heating in mineral oil to induce a morphological transition.³⁴

SAXS is a powerful structural characterization technique for colloidal dispersions. It can provide detailed information on particle size, morphology, and interparticle interactions.³⁶ SAXS patterns recorded for 1.0% w/w dispersions of the linear S_{31} – B_{200} spheres and core cross-linked S_{31} – B_{200} – E_{20} spheres in mineral oil are shown in Figure 2d. In both cases the low q region has a gradient of approximately zero, as expected

for non-interacting spheres. The SAXS patterns could be fitted using a well-known spherical micelle model (see dashed white traces in Figure 2d).³⁵ This model indicated core diameters of 27.6 ± 2.1 and 29.4 ± 2.4 nm and mean aggregation numbers of 218 and 234 for the linear and core cross-linked nanoparticles, respectively (see Table S1 for summary of fitting parameters). Importantly, the SAXS pattern obtained at 100 °C for the same 1.0% w/w dispersion of S_{31} - B_{200} - E_{20} spheres in mineral oil is essentially identical to that collected at 25 °C (see Figure 2d).

Liu and co-workers reported³ that their acrylic core cross-linked spherical nanoparticles enhanced the lubricant performance of a Group II base oil. More specifically, a significant reduction in the friction coefficient was observed in the boundary lubrication regime at low entrainment speeds when constructing Stribeck curves using a mini-traction machine (MTM). According to Zheng et al.,³ the spherical nanoparticles are drawn into the asperity contact area, where they undergo elastic deformation and hence prevent direct contact between the two moving surfaces. This so-called “ball-bearing” effect has also been proposed for spherical inorganic nanoparticle additives.^{37,38} In the present study, we utilize precisely the same experimental conditions to assess the lubricating performance of the cross-linked S_{31} - B_{200} - E_{20} spheres prepared directly in a Group III base oil.

In an MTM experiment, the friction generated between the rotating steel ball and disk is manifested as the maximum force that can be applied before slippage is observed. The relationship between the friction coefficient (μ_f), friction force (F_f), and the normal force (F_n) is given by $F_f = \mu_f F_n$.

Glyceryl monooleate (GMO) is widely used as a friction modifier for automotive engine oil formulations.³⁹ When present at 0.5% w/w, this additive reduces the friction coefficient of the base oil within the boundary lubrication regime. However, using 0.5% w/w core cross-linked S_{31} - B_{200} - E_{20} spheres of 48 nm diameter clearly leads to a much more dramatic reduction in the friction coefficient at entrainment speeds below 50–60 mm s^{-1} . Indeed, the Stribeck curve shown in Figure 3 is strikingly similar to that reported by Liu and co-workers³ when using 0.5% w/w cross-linked acrylic copolymer spheres of 35 nm diameter under the same

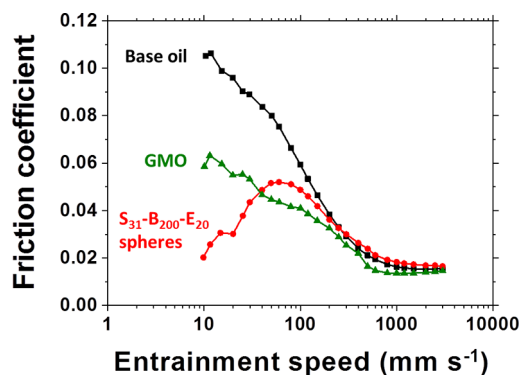


Figure 3. Stribeck curves showing the change in friction coefficient with entrainment speed for a lubricating base oil alone (black squares), for 0.5% w/w glyceryl monooleate (GMO, green triangles) in the same base oil, and for a 0.5% w/w dispersion of 48 nm diameter S_{31} - B_{200} - E_{20} spheres dispersed in the same base oil (red circles). Data were recorded at a 20% slide-to-roll ratio (SRR) under an applied load of 35 N at 100 °C.

operating conditions. At an entrainment speed of 10 mm s^{-1} , the friction coefficient observed for the S_{31} - B_{200} - E_{20} spheres is approximately 0.02, which is a remarkably low value. Importantly, the addition of 0.5% w/w S_{31} - B_{200} - E_{20} spheres results in a negligible change in the solution viscosity at both 25 and 100 °C compared to mineral oil. Moreover, the nanoparticle dispersion exhibited Newtonian rheological behavior at both temperatures (see Figure S3).

RAFT polymerization was developed by Rizzardo and co-workers, who have demonstrated its versatility and excellent tolerance of a wide range of monomer functionality.^{40–42} However, one important barrier to commercialization of formulations and processes based on this chemistry is the organosulfur-based RAFT agent, which confers both color and malodor.^{43,44} In principle, the RAFT chain-ends can be removed via several routes including the addition of excess initiator.^{45,46} Moreover, this post-polymerization modification can be achieved for block copolymer nanoparticles.²⁹ However, such derivatization is unlikely to be cost-effective for many industrial applications.^{43,44} It is perhaps worth emphasizing in this context that commercial engine and gear oils typically already contain low levels of organosulfur-based additives; indeed, scientists at the Lubrizol Corporation have already demonstrated that RAFT end-groups can be tolerated in star copolymers designed to act as viscosity modifiers for such fluids.^{47,48}

CONCLUSIONS

In summary, the methacrylic core cross-linked spheres reported herein offer excellent boundary lubrication performance. Given their highly convenient synthesis via RAFT dispersion polymerization and bearing in mind that RAFT end-group removal is not required for this particular application, these nanoparticles appear to be well-suited for the formulation of next-generation ultralow-viscosity automotive engine oils that significantly reduce friction in the boundary lubrication regime, thus delivering enhanced energy efficiency (i.e., greater fuel economy).

ASSOCIATED CONTENT

Supporting Information

The Supporting Information is available free of charge on the ACS Publications website at DOI: 10.1021/acsami.9b12472.

¹H NMR spectra; TEM study of cross-linked nanoparticles dispersed in THF; SAXS data for cross-linked nanoparticles dispersed in mineral oil at 25 and 100 °C; SAXS models (PDF)

AUTHOR INFORMATION

Corresponding Authors

*E-mail: m.derry@sheffield.ac.uk. Phone: +44(0)114-222-9503.

*E-mail: s.p.arnes@sheffield.ac.uk. Phone: +44(0)114-222-9342.

ORCID

Matthew J. Derry: 0000-0001-5010-6725

Steven P. Arnes: 0000-0002-8289-6351

Notes

The authors declare no competing financial interest.

ACKNOWLEDGMENTS

The Lubrizol Corporation is thanked for funding a Ph.D. studentship for M.J.D. and for permission to publish this work. S.P.A. acknowledges EPSRC for an Established Career Particle Technology Fellowship (EP/R003009). Zahra Hussain (The Lubrizol Corporation) is thanked for the lubricity data reported in this study.

REFERENCES

- (1) Covitch, M. J.; Brown, M.; May, C.; Selby, T.; Goldmints, I.; George, D. Extending SAE J300 to Viscosity Grades below SAE 20. *SAE International Journal of Fuels and Lubricants* **2010**, *3*, 1030–1040.
- (2) Fink, J. K. Chapter 3—Thickeners. In *Hydraulic Fracturing Chemicals and Fluids Technology*; Gulf Professional Publishing: Houston, TX, 2013; pp 35–57.
- (3) Zheng, R.; Liu, G.; Devlin, M.; Hux, K.; Jao, T.-C. Friction reduction of lubricant base oil by micelles and crosslinked micelles of block copolymers. *Tribol. Trans.* **2009**, *53*, 97–107.
- (4) Holmberg, K.; Andersson, P.; Erdemir, A. Global energy consumption due to friction in passenger cars. *Tribol. Int.* **2012**, *47*, 221–234.
- (5) Ali, M. K. A.; Xianjun, H. Improving the tribological behavior of internal combustion engines via the addition of nanoparticles to engine oils. *Nanotechnol. Rev.* **2015**, *4*, 347–358.
- (6) Zheng, R.; Liu, G.; Jao, T.-C. Poly (2-ethylhexyl acrylate)-ran-(tert-butyl acrylate) -block-poly(2-cinnamoyloxyethyl acrylate) synthesis and properties. *Polymer* **2007**, *48*, 7049–7057.
- (7) Heywood, J. B. *Internal Combustion Engine Fundamentals*; McGraw-Hill Book Co.: Singapore, 1988.
- (8) *Standard Test Method for Determination of Additive Elements in Lubricating Oils by Inductively Coupled Plasma Atomic Emission Spectrometry*; ASTM International, 2014; ASTM D4951.
- (9) Warren, N. J.; Armes, S. P. Polymerization-induced self-assembly of block copolymer nano-objects via RAFT aqueous dispersion polymerization. *J. Am. Chem. Soc.* **2014**, *136*, 10174–10185.
- (10) Derry, M. J.; Fielding, L. A.; Armes, S. P. Polymerization-induced self-assembly of block copolymer nanoparticles via RAFT non-aqueous dispersion polymerization. *Prog. Polym. Sci.* **2016**, *52*, 1–18.
- (11) Canning, S. L.; Smith, G. N.; Armes, S. P. A critical appraisal of RAFT-mediated polymerization-induced self-assembly. *Macromolecules* **2016**, *49*, 1985–2001.
- (12) Pei, Y.; Lowe, A. B.; Roth, P. J. Stimulus-responsive nanoparticles and associated (reversible) polymorphism via polymerization induced self-assembly (PISA). *Macromol. Rapid Commun.* **2017**, *38*, 1600528.
- (13) Wan, W.-M.; Hong, C.-Y.; Pan, C.-Y. One-pot synthesis of nanomaterials via RAFT polymerization induced self-assembly and morphology transition. *Chem. Commun.* **2009**, 5883–5885.
- (14) He, W.-D.; Sun, X.-L.; Wan, W.-M.; Pan, C.-Y. Multiple morphologies of PAA-b-PSt assemblies throughout RAFT dispersion polymerization of styrene with PAA macro-CTA. *Macromolecules* **2011**, *44*, 3358–3365.
- (15) Jones, E. R.; Semsarilar, M.; Blanz, A.; Armes, S. P. Efficient synthesis of amine-functional diblock copolymer nanoparticles via RAFT dispersion polymerization of benzyl methacrylate in alcoholic media. *Macromolecules* **2012**, *45*, 5091–5098.
- (16) Zehm, D.; Ratcliffe, L. P. D.; Armes, S. P. Synthesis of diblock copolymer nanoparticles via RAFT alcoholic dispersion polymerization: Effect of block copolymer composition, molecular weight, copolymer concentration, and solvent type on the final particle morphology. *Macromolecules* **2013**, *46*, 128–139.
- (17) Zhang, W. J.; Hong, C. Y.; Pan, C. Y. Fabrication of spaced concentric vesicles and polymerizations in RAFT dispersion polymerization. *Macromolecules* **2014**, *47*, 1664–1671.
- (18) Gonzato, C.; Semsarilar, M.; Jones, E. R.; Li, F.; Krooshof, G. J. P.; Wyman, P.; Mykhaylyk, O. O.; Tuinier, R.; Armes, S. P. Rational synthesis of low-polydispersity block copolymer vesicles in concentrated solution via polymerization-induced self-assembly. *J. Am. Chem. Soc.* **2014**, *136*, 11100–11106.
- (19) Pei, Y.; Lowe, A. B. Polymerization-induced self-assembly: Ethanolic RAFT dispersion polymerization of 2-phenylethyl methacrylate. *Polym. Chem.* **2014**, *5*, 2342–2351.
- (20) Pei, Y.; Dharsana, N. C.; Lowe, A. B. Ethanolic RAFT dispersion polymerization of 2-(naphthalen-2-yloxy)ethyl methacrylate and 2-phenoxyethyl methacrylate with poly[2-(dimethylamino)-ethyl methacrylate] macro-chain transfer agents. *Aust. J. Chem.* **2015**, *68*, 939–945.
- (21) Pei, Y. W.; Noy, J. M.; Roth, P. J.; Lowe, A. B. Thiol-reactive Passerini-methacrylates and polymorphic surface functional soft matter nanoparticles via ethanolic RAFT dispersion polymerization and post-synthesis modification. *Polym. Chem.* **2015**, *6*, 1928–1931.
- (22) Fielding, L. A.; Derry, M. J.; Admiral, V.; Rosselgong, J.; Rodrigues, A. M.; Ratcliffe, L. P. D.; Sugihara, S.; Armes, S. P. RAFT dispersion polymerization in non-polar solvents: Facile production of block copolymer spheres, worms and vesicles in n-alkanes. *Chemical Science* **2013**, *4*, 2081–2087.
- (23) Fielding, L. A.; Lane, J. A.; Derry, M. J.; Mykhaylyk, O. O.; Armes, S. P. Thermo-responsive diblock copolymer worm gels in non-polar solvents. *J. Am. Chem. Soc.* **2014**, *136*, 5790–5798.
- (24) Lopez-Oliva, A. P.; Warren, N. J.; Rajkumar, A.; Mykhaylyk, O. O.; Derry, M. J.; Doncom, K. E. B.; Rymaruk, M. J.; Armes, S. P. Polydimethylsiloxane-based diblock copolymer nano-objects prepared in nonpolar media via RAFT-mediated polymerization-induced self-assembly. *Macromolecules* **2015**, *48*, 3547–3555.
- (25) Pei, Y.; Sugita, O. R.; Thurairajah, L.; Lowe, A. B. Synthesis of poly(stearyl methacrylate-b-3-phenylpropyl methacrylate) nanoparticles in n-octane and associated thermoreversible polymorphism. *RSC Adv.* **2015**, *5*, 17636–17646.
- (26) Pei, Y.; Thurairajah, L.; Sugita, O. R.; Lowe, A. B. RAFT dispersion polymerization in nonpolar media: Polymerization of 3-phenylpropyl methacrylate in n-tetradecane with poly(stearyl methacrylate) homopolymers as macro chain transfer agents. *Macromolecules* **2015**, *48*, 236–244.
- (27) Pei, Y.; Noy, J.-M.; Roth, P. J.; Lowe, A. B. Soft matter nanoparticles with reactive coronal pentafluorophenyl methacrylate residues via non-polar RAFT dispersion polymerization and polymerization-induced self-assembly. *J. Polym. Sci., Part A: Polym. Chem.* **2015**, *53*, 2326–2335.
- (28) Ratcliffe, L. P. D.; McKenzie, B. E.; Le Bouëdec, G. M. D.; Williams, C. N.; Brown, S. L.; Armes, S. P. Polymerization-Induced Self-Assembly of All-Acrylic Diblock Copolymers via RAFT Dispersion Polymerization in Alkanes. *Macromolecules* **2015**, *48*, 8594–8607.
- (29) Cornel, E. J.; van Meurs, S.; Smith, T.; O’Hora, P. S.; Armes, S. P. In situ spectroscopic studies of highly transparent nanoparticle dispersions enable assessment of trithiocarbonate chain-end fidelity during RAFT dispersion polymerization in nonpolar media. *J. Am. Chem. Soc.* **2018**, *140*, 12980–12988.
- (30) Derry, M. J.; Fielding, L. A.; Armes, S. P. Industrially-relevant polymerization-induced self-assembly formulations in non-polar solvents: RAFT dispersion polymerization of benzyl methacrylate. *Polym. Chem.* **2015**, *6*, 3054–3062.
- (31) Derry, M. J.; Fielding, L. A.; Warren, N. J.; Mable, C. J.; Smith, A. J.; Mykhaylyk, O. O.; Armes, S. P. In situ small-angle X-ray scattering studies of sterically-stabilized diblock copolymer nanoparticles formed during polymerization-induced self-assembly in non-polar media. *Chemical Science* **2016**, *7*, 5078–5090.
- (32) Rymaruk, M. J.; Hunter, S. J.; O’Brien, C. T.; Brown, S. L.; Williams, C. N.; Armes, S. P. RAFT Dispersion Polymerization in Silicone Oil. *Macromolecules* **2019**, *52*, 2822–2832.
- (33) Derry, M. J.; Mykhaylyk, O. O.; Ryan, A. J.; Armes, S. P. Thermoreversible crystallization-driven aggregation of diblock copolymer nanoparticles in mineral oil. *Chemical Science* **2018**, *9*, 4071–4082.

- (34) Derry, M. J.; Mykhaylyk, O. O.; Armes, S. P. A vesicle-to-worm transition provides a new high-temperature oil thickening mechanism. *Angew. Chem., Int. Ed.* **2017**, *56*, 1746–1750.
- (35) Pedersen, J. S. Form factors of block copolymer micelles with spherical, ellipsoidal and cylindrical cores. *J. Appl. Crystallogr.* **2000**, *33*, 637–640.
- (36) Narayanan, T.; Wacklin, H.; Konovalov, O.; Lund, R. Recent applications of synchrotron radiation and neutrons in the study of soft matter. *Crystallogr. Rev.* **2017**, *23*, 160–226.
- (37) Wu, Y. Y.; Tsui, W. C.; Liu, T. C. Experimental analysis of tribological properties of lubricating oils with nanoparticle additives. *Wear* **2007**, *262*, 819–825.
- (38) Lee, K.; Hwang, Y.; Cheong, S.; Choi, Y.; Kwon, L.; Lee, J.; Kim, S. H. Understanding the Role of Nanoparticles in Nano-oil Lubrication. *Tribol. Lett.* **2009**, *35*, 127–131.
- (39) Spikes, H. Friction Modifier Additives. *Tribol. Lett.* **2015**, *60*, 5.
- (40) Chiefari, J.; Chong, Y. K.; Ercole, F.; Krstina, J.; Jeffery, J.; Le, T. P. T.; Mayadunne, R. T. A.; Meijs, G. F.; Moad, C. L.; Moad, G.; Rizzardo, E.; Thang, S. H. Living free-radical polymerization by reversible addition-fragmentation chain transfer: The RAFT process. *Macromolecules* **1998**, *31*, 5559–5562.
- (41) Moad, G.; Rizzardo, E.; Thang, S. H. Living radical polymerization by the RAFT process. *Aust. J. Chem.* **2005**, *58*, 379–410.
- (42) Moad, G.; Rizzardo, E.; Thang, S. H. Living Radical Polymerization by the RAFT Process - A Second Update. *Aust. J. Chem.* **2009**, *62*, 1402–1472.
- (43) Perrier, S. 50th Anniversary Perspective: RAFT Polymerization—A User Guide. *Macromolecules* **2017**, *50*, 7433–7447.
- (44) Destarac, M. Industrial development of reversible-deactivation radical polymerization: is the induction period over? *Polym. Chem.* **2018**, *9*, 4947–4967.
- (45) Perrier, S.; Takolpuckdee, P. Macromolecular design via reversible addition-fragmentation chain transfer (RAFT)/Xanthates (MADIX) polymerization. *J. Polym. Sci., Part A: Polym. Chem.* **2005**, *43*, 5347–5393.
- (46) Willcock, H.; O'Reilly, R. K. End group removal and modification of RAFT polymers. *Polym. Chem.* **2010**, *1*, 149–157.
- (47) Brzytwa, A. J.; Johnson, J. Scaled Production of CTA—A Star Performer. *Polym. Prepr. (Am. Chem. Soc., Div. Polym. Chem.)* **2011**, *52* (2), 533–534.
- (48) Baum, M.; Schober, B. J.; Davies, M. C.; Viger, D. C.; Johnson, J. R. *Process for Preparing Polymers and Compositions Thereof*. U.S. Patent 20130310291A1, 2013.